Multilevel Power Transfer Function Characterization of Nonlinear Optical Loop Mirror

Feng Wen*[1,2], Stylianos Sygletos[1], Christos P. Tsekrekos[1], Xingyu Zhou[2], Yong Geng[2], Baojian Wu[2], Kun Qiu[2], and Sergei K. Turitsyn[1]

[1]*Aston Institute of Photonic Technologies, Aston University, B4 7ET Birmingham, UK*

[2]*Key Lab of Optical Fiber Sensing and Communication Networks, Ministry of Education, University of Electronic Science and Technology of China, 611731 Chengdu, China*

f.wen@aston.ac.uk

ABSTRACT

The power transfer function of a nonlinear optical loop mirror (NOLM) is experimentally investigated for both continuous-wave and pulsed operation of the pump signal. The difference between transmission and reflection responses is discussed in view of using the interferometer for the amplitude regeneration of multilevel signals.

Keywords: nonlinear optical loop mirror, power transfer function, all-optical amplitude regenerator.

1. INTRODUCTION

All-optical multilevel regeneration of optical signals can open up drastically different approaches to the design of high-capacity telecommunications links. The potential of the nonlinear optical loop mirror (NOLM) to act as an amplitude regenerator for conventional two-level (binary) signals has been known for many years [1]. Facing the rapid development of advanced modulation signals in commercial communication networks, the new challenge is to design NOLM-based subsystems for regenerating a higher number of levels. By adopting a bidirectional Erbium-doped fibre amplifier (Bi-EDFA), the amplitude regeneration for a return-to-zero differential quadrature phase-shift keying (RZ-DQPSK) signal was demonstrated [2]. In an attenuation-imbalanced NOLM, two-level amplitude regeneration was experimentally achieved for a RZ star-8 quadrature amplitude modulated (RZ star-8QAM) signal [3]. A NOLM-based phase sensitive amplifier has been used in [4] to demonstrate the phase-and-amplitude regeneration for a RZ-DPSK signal. Furthermore, multilevel-amplitude and -phase regeneration have been also theoretically investigated in a nonlinear amplifying loop mirror (NALM) [5] and a coupled NOLM architecture [6].

High effective powers in the NOLM are crucial to achieve the large nonlinear phase shifts that are required for multilevel operation. However, in typical highly nonlinear fibres (HNLFs) stimulated Brillouin scattering effects (SBS) introduce major limitations for such operation. The SBS threshold can be increased either with the use of pulsed pump signals [2]-[4] or by applying strain or temperature distribution along the HNLF [7]-[9]. In this paper, a strained HNLF was used and we compared the power transfer function (PTF) response for continuous-wave (CW) and pulsed-pump operation. The experimental results were well matched to the results of the numerical model, which was developed to explore in more detail the operation parameters of the regenerator. Experimental and theoretical results show that for pulsed pump operation four power plateau regions were obtained.

2. THEORY

NOLM interferometer creates a phase difference between the co- and counter-propagating signals using the Kerr effect. The development of the theoretical model was based on the setup of Fig. 1(a). The NOLM was composed by an optical coupler (OC), a power tuning (PT) device and a HNLF. The PT device could be a variable optical attenuator (VOA) – just as in our experiment – for introducing the extra inner loss, or a Bi-EDFA [5]. The transmission light was obtained from the Out-port of optical coupler, and the reflected light was collected at the P3 port of optical circulator (CIR). Following the methodology of [10,11], the transmission power P_{out}^{Ref} and reflection power P_{out}^{Tra} of the NOLM can be derived as a function of the corresponding input signal powers P_{in}^{Ref} and P_{in}^{Tra} :

$$\begin{cases} P_{out}^{Ref} = 2C_P\beta(1-\beta)\left(1+\cos\Phi_\beta\right)P_{in}^{Ref} \\ P_{out}^{Tra} = C_P\left[1-2\beta(1-\beta)\left(1+\cos\Phi_\beta\right)\right]P_{in}^{Tra} \end{cases} \tag{1}$$

where the power tuning parameter $C_P = \exp(2s\delta - \alpha L)$ is determined by the PT device and the HNLF parameters, with s = ± 1 corresponding to amplification or attenuation, δ is the PT coefficient, α and L are the loss and length of the HNLF. The nonlinear phase difference between the co- and counter- propagating signals is given by the $\Phi_\beta = \gamma L\left[\exp(2s\delta)(1-\beta)-\beta\right]P_{in}^{i}$ where β is the splitting ratio of optical coupler, and γ is the nonlinear coefficient of the fibre.

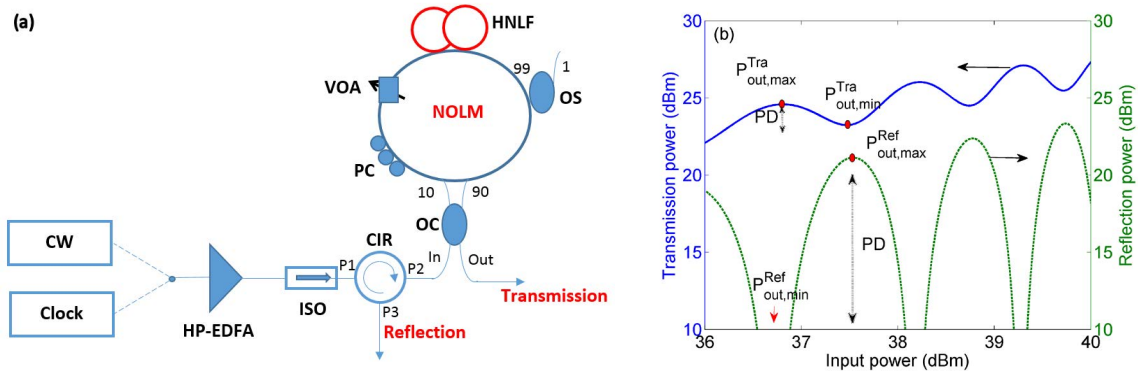

Figure 1: (a) Setup of the NOLM; (b) Corresponding power transfer function (PTF) curves.

Equation 1 and Fig. 1(b), reveal the oscillatory nature of the NOLM's transfer function, characterized by local max and min output power values for each oscillation period. Multiple power plateau regions are observed in both transmission and reflection ports. For multilevel operation each input signal level should be set within the plateau region that is centred around the input power $P^{i}_{in,\max}$ with (i = *Ref or Tra*) where the local max output power $P^{i}_{out,\max}$ is obtained. Moreover, for the transmission port the best performance is achieved when the power difference (PD) = $P^{i}_{out,\max} - P^{i}_{out,\min}$ is minimized. The plateau locations can be roughly estimated by solving the equation $1+\cos\Phi_{\beta} = 0$ or 2 as function of the input power. For the reflection port, the solutions are:

$$\begin{cases} P^{Ref}_{out,\max} = 4C_P\beta(1-\beta)\cdot P^{Ref}_{in,\max} & P^{Ref}_{in,\max} = \dfrac{2m\pi}{\gamma L\left[\exp(2s\delta)(1-\beta)-\beta\right]} \\ P^{Ref}_{out,\min} = 0 & P^{Ref}_{in,\min} = \dfrac{(2m+1)\pi}{\gamma L\left[\exp(2s\delta)(1-\beta)-\beta\right]} \end{cases} \tag{2}$$

whereas for the transmission port, we get:

$$\begin{cases} P^{Tra}_{out,\max} = C_P\cdot P^{Tra}_{in,\max} & P^{Tra}_{in,\max} = \dfrac{(2m+1)\pi}{\gamma L\left[\exp(2s\delta)(1-\beta)-\beta\right]} \\ P^{Tra}_{out,\min} = C_P\left[1-4\beta(1-\beta)\right]\cdot P^{Tra}_{in,\min} & P^{Tra}_{in,\min} = \dfrac{2m\pi}{\gamma L\left[\exp(2s\delta)(1-\beta)-\beta\right]} \end{cases} \tag{3}$$

The calculated power difference is larger for the reflection port rather than the transmission port, suggesting a less efficient regenerative performance. Meanwhile, the optimum operating conditions are also a function of the interferometer parameters β and δ, which gives the opportunity to identify associated trade-offs for more power efficient operation.

3. EXPERIMENT

To investigate the PTF experimentally, a CW light source at 1550 nm wavelength and a 10 GHz optical clock (optical pulse train) with a pulse width around 10 ps have been used in two separate experimental scenarios, as shown in Fig. 1(a). In both cases a high power EDFA (HP-EDFA) amplified the signal to 36.5 dBm. An optical isolator prevented unwanted feedback light to the optical transmitter. The NOLM unit included a 90:10 optical coupler, a 99:1 optical splitter (OS), a 606 m-length strained aluminous-silicate HNLF, a variable optical attenuator and a polarization controller (PC). At the input port, an optical circulator was used to obtain the reflection signal. According to the theoretical analysis, an OC of 90:10 splitting ratio was required to enable a large nonlinear phase difference between the two arms of the interferometer for multilevel operation. At the 1% output port of the OS, the exact input power to the NOLM was measured. The nonlinear medium was a strained HNLF of increased stimulated Brillouin scattering (SBS) threshold and a nonlinear coefficient γ of 7 W^{-1}/km. The use of the VOA in the loop enabled further adjustment of the power levels of the two counter-propagating waves. Before stimulating the nonlinear response induced by Kerr effects, the polarization controller was used to adjust the birefringence bias for the NOLM unit, and for our experiment the initial state corresponded to the lowest reflection power in the linear operation. The reflection and transmission light were obtained from the Out-port of optical coupler and the P3 port of optical circulator, respectively.

Initially we launched a CW light into the NOLM and characterized the power transfer function of the reflection port, see Fig. 2(a). Theoretical PTF curves, using the aforementioned model, were also obtained and matched to the experimental data. When the input power was less than 23 dBm experiment and theory was in good agreement. However, by increasing further the input power, the reflected power was dramatically increased due

to the SBS effect, and the power plateau predicted by theory couldn't be achieved. Tuning the VOA to introduce an extra inner loss to the NOLM reduced accordingly the reflected power when the input power level was low. However, for high input power levels, such as 33 dBm, a fixed amount of reflected power was measured independently of the VOA induced loss, which means that the reflected light was coming from the SBS effect rather than the interference process.

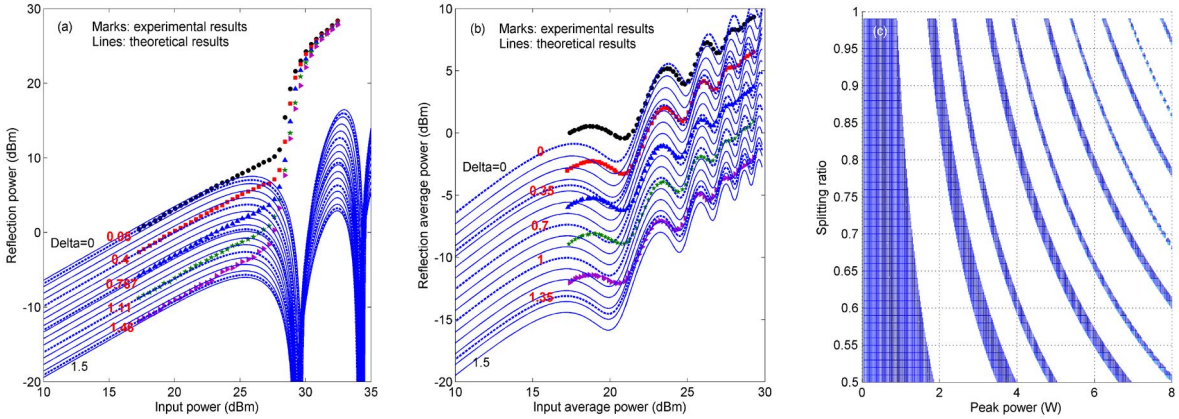

Figure 2. Reflection PTFs with the increase of PT coefficients δ for: (a) CW light input and (b) pulse signal input; (c) Slope result of less than 1 with different splitting ratios and pulse peak powers.

When the optical clock was input into the NOLM unit, the nonlinear PTF curve was obtained, see Fig. 2(b). Four power plateau regions were observed at the first time due to a higher nonlinear response. The local max and min output powers were shifted with the inner loss, just as it was predicted by our theoretical model. To match with the experimental results, PT coefficients of 0, 0.35, 0.7, 1 and 1.35 were used in the simulation. The difference between experimental and theoretical results was attributed to the fibre dispersion effect which was ignored in our model. Comparing to the CW case, the multilevel PTF curve was smoother for the pulsed input, thus suitable for amplitude regeneration. To determine the operation range for the different amplitude levels, the slope of the PTF curve was calculated and depicted in Fig. 2(c). The blue coloured regions correspond to absolute slope values of less than 1 on the logarithmic PTF, where amplitude noise suppression takes place. A wide operation range suitable for the regeneration of BPSK or QPSK signals was achieved for the first power plateau region, whereas higher order plateaus become significantly narrower.

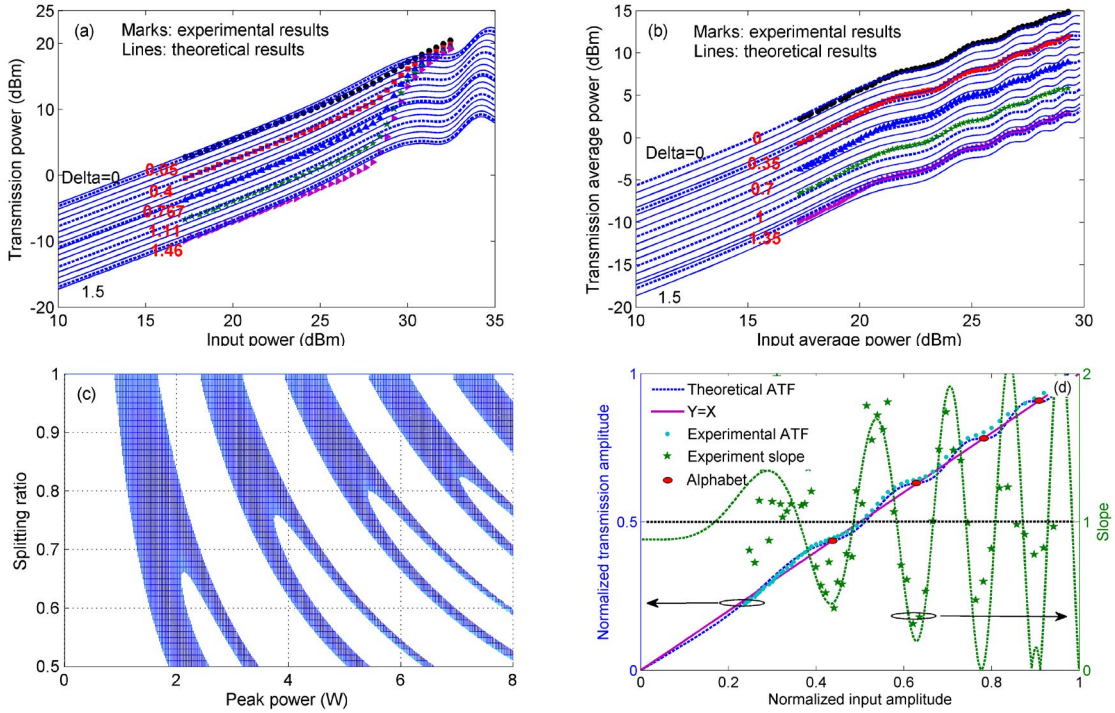

Figure 3. Transmission PTFs with the increase of PT coefficients δ for: (a) CW light input and (b) pulse signal input; (c) Slope result of less than 1 with different splitting ratios and pulse peak powers; (d) Normalized amplitude transfer function (ATF) and its slope.

Similar tests were carried out for the transmission port, and the corresponding results are depicted in Fig. 3. For the CW case, good agreement between theory and experiment was obtained below the SBS threshold and for PT coefficients equal to 0.05, 0.4, 0.767, 1.11 and 1.46. At high input power levels, due to the SBS impact the output power of the transmission port converged to a single fixed value with no plateau regions being observed. On the other hand, when having the optical clock as input signal to the NOLM, a multilevel regenerative PTF was observed, similar to the reflection case of Fig. 2(b), but with smoother curves. In this transfer function four power plateau regions were achieved, which potentially makes it suitable for the regeneration of PAM4 and circular 64QAM signals. To demonstrate regeneration regions, the slope was calculated on the logarithmic PTF as depicted in Fig. 3(c). It can be seen that large splitting ratios move the regenerative levels to lower input powers. Also similar plateau widths were calculated when the splitting ratio was higher than 0.9, offering an equal noise handling capability for each regenerative level. In Fig. 3(d), the amplitude transfer function (ATF) was extrapolated directly from the PTF when no extra inner loss was induced by the VOA. Four alphabet points at the centre of the plateau regions were successfully obtained satisfying the definition of [12], which prevents the linear distortion of the input constellation levels and makes the regenerator suitable an in-line cascaded operation.

4. CONCLUSIONS

In this paper, the PTF performance of a NOLM unit was investigated for CW- and pulsed-pump power operation. A theoretical model was derived based on our experiment setup, and the operation points and the ranges of the plateau regions on the PTF curves were discussed. Nonlinear power responses with four plateau regions were achieved for the both reflection and transmission ports for pulsed pump input. On the contrary, SBS effects prevented similar performance for CW pump signals. Good agreement between experimental and theoretical results was obtained below the SBS threshold. Through introducing an additional inner loss factor the operation power could be further tuned to match with input signals. Wide operation ranges, defined by slope values of less than 1, were observed for the transmission response.

ACKNOWLEDGEMENTS

The authors would like to thank Tyndall National Institute for the loan of the highly nonlinear fibre, and Mariia Sorokina, Ian Phillips, Marc Stephens, Fillipe Ferreira, MingMing Tan, Lukasz Krzczanowicz for the valuable discussions about the experiment. This work has been supported by the EPSRC projects UNLOC (EP/J017582/1), the Marie Sklodowska-Curie Action (701770-INNOVATION), the National Natural Science Foundation of China (61505021, 61671108, 61271166), and the Program for Changjiang Scholars and Innovative Research Team in Universities of China (IRT1218), the 111 Project (B14039).

REFERENCES

[1] N. J. Doran and D. Wood: Nonlinear-optical loop mirror, *Opt. Lett.,* vol. 13. pp. 56-58, Jan. 1988.
[2] K. Cvecek *et al.*: 2R-regeneration of an 80-Gb/s RZ-DQPSK signal by a nonlinear amplifying loop mirror, *IEEE Photon. Technol. Lett.*, vol. 19. pp. 1475-1477, Oct. 2007.
[3] T. Roethlingshoefer *et al.*: All-optical phase-preserving multilevel amplitude regeneration, *Opt. Express,* vol. 22. pp. 27077-27085, Nov. 2014.
[4] K. Croussore *et al.*: Phase-and-amplitude regeneration of differential phase-shift keyed signals using a phase-sensitive amplifier, *Opt. Express,* vol. 14. pp. 2085-2094, Mar. 2006.
[5] T. Roethlingshoefer *et al.*: Cascaded phase-preserving multilevel amplitude regeneration, *Opt. Express,* vol. 22. pp. 31729-31734, Dec. 2014.
[6] M. Sorokina: Design of multilevel amplitude regenerative system, *Opt. Lett.,* vol. 39. pp. 2499-2502, Apr. 2014.
[7] L. Grüner-Nielsen *et al.*: Silica-based highly nonlinear fibers with a high SBS threshold, in *Proc. IEEE Photonics Society 2011 Winter Topical Meeting*, Keystone, America, Jan. 2011, paper MD3.2.
[8] M. Takahashi *et al.*: Dispersion and Brillouin managed HNLFs by strain control techniques, *J. Lightw. Technol.,* vol. 28. pp. 59-64, Jan. 2010.
[9] J. Hansryd *et al.*: Increase of the SBS threshold in a short highly nonlinear fiber by applying a temperature distribution, *J. Lightw. Technol.,* vol. 19. pp. 1691-1697, Nov. 2001.
[10] K. Croussore *et al.*: All-Optical regeneration of differential phase-shift keyed signals based on phase-sensitive amplification, in *Proc. SPIE 2005*, Bellingham, America, Jun. 2005, paper 166.
[11] F. Wen *et al.*: All-fiber magneto-optic Sagnac interferometer, *Appl. Opt.,* vol. 50. pp. 3123-3127, Jul. 2011.
[12] M. A. Sorokina and S. K. Turitsyn: Regeneration limit of classical Shannon capacity, *Nat. Commun.,* vol. 5. p. 3861, May 2014.